Effects of Various Factors on Durability Prediction of Nuclear Waste Containment Structures - 11546

Sohini Sarkar[1], David S. Kosson[1], Sankaran Mahadevan[1], Hans Meeussen[2], Hans van der Sloot[3], Kevin G. Brown[1], Greg Flach[4], Christine Langton[4]

[1] Vanderbilt University, Nashville, TN, USA
[2] Nuclear Research and Consultancy Group, Petten, The Netherlands
[3] Hans van der Sloot Consultancy, The Netherlands
[4] Savannah River National Laboratory, Aiken, SC, USA

ABSTRACT

A numerical methodology is presented in this paper to simulate the degradation of concrete vaults exposed to aggressive sulfate-containing pore solution of the low activity nuclear wastes. The methodology incorporates (i) transport of ions, (ii) chemical reactions, and (iii) damage accumulation due to cracking. The required parameters and boundary conditions for simulating structural damage are generally obtained from literature and experiments. Parameters that cannot be directly measured in experiments are often estimated using measurable quantities and empirical relations. Uncertainty in inputs, model parameters and boundary conditions due to inherent randomness, lack of data and incomplete knowledge of the physics introduces uncertainty in the model prediction, which is evaluated using sensitivity analysis and Monte Carlo simulation. This paper investigates the effects of three primary factors on the model prediction. These are – (1) chemical equilibrium models comprised of different combinations of mineral phases and initial concentrations of ionic species, (2) prescribed boundary conditions, and (3) a mechanical parameter required for initiation and propagation of cracking.

The numerical model is then used to assess durability of a concrete containment structure considering uncertainty in the selected physical and chemical parameters. Various approaches for statistical representation of the uncertainties are incorporated in the durability assessment framework. Finally, the probability distribution of time to structural damage is evaluated using a single loop Monte Carlo simulation technique.

INTRODUCTION

Low activity nuclear waste is being disposed by mixing with cementitious materials and then being placed in above ground reinforced concrete vaults which are to be covered with soil and a final cap to achieve a shallow burial scenario for final disposition. The waste materials contain various salts of sulfate, carbonate, chloride, nitrite, etc. Sulfate attack from sulfate contained in

the waste form has been identified to be one of the potentially important degradation mechanisms for the reinforced concrete containment structures [1]. Thus it is important to assess the durability of such structures subjected to aggressive conditions so that engineered systems can be designed such that long-term degradation of contaminant retention structures is minimized and contaminant release rates and extents do not exceed acceptable levels.

When sulfate ions diffuse through a structure, they react with the cement hydration products to form expansive products. This induces strain leading to cracking and eventual failure. The numerical model developed for the purpose of durability assessment incorporates the three stages of the degradation process – diffusion of ions, chemical reactions and damage accumulation due to cracking. There are several input and model parameters in these three parts of the model. The effects of these parameters on the durability analysis are assessed using the numerical model. Finally, the integrated effect of physical and chemical parameter uncertainty is quantified by performing probabilistic durability analysis using a single loop Monte Carlo simulation technique.

NUMERICAL MODELING FRAMEWORK

The numerical model used in this paper incorporates three essential stages of degradation of cement-based structures – diffusion of ions, chemical reactions and damage accumulation. Brief descriptions of the stages are given in the following subsections. Detailed descriptions of the following approaches are given in [2].

Diffusion of ions

Assuming the structure to be saturated, porous and under isothermal condition, the governing equation for diffusion of an ion is expressed as

$$\frac{\partial(\varphi c_i)}{\partial t} = \mathrm{div}\left(\frac{D_i^0 \varphi}{\tau}\left(\mathrm{grad}(c_i) + c_i\,\mathrm{grad}(\ln \gamma_i)\right)\right) \qquad (1)$$

where c_i is the concentration of the i^{th} ion, D_i^0 is the free solution diffusivity of the ion, φ is the porosity, τ is the tortuosity and γ_i is the chemical activity coefficient of the ion. The modified Davies equation [3] is used to calculate the chemical activity of the ions, which produces better results for highly concentrated ionic solutions such as concrete pore solutions than other formulations of activity coefficient [4].

Chemical reactions

Some of the main hydration products which are generally present in a matured cement-based structure are calcium silicate hydrate (CSH), calcium hydroxide or Portlandite (CH), ettringite

($C_6A\bar{S}_3H_{32}$), calcium monosulfoaluminate ($C_4A\bar{S}H_{12}$), hydrogarnet (C_3AH_6), etc. When sulfate ions diffuse through a structure, a series of reactions take place. If the diffusing species is sodium sulfate, it reacts with Portlandite to form gypsum and with calcium monosulfate and tricalcium aluminate to form ettringite. The gypsum can then react with any of the calcium aluminate phases, e.g. calcium monosulfate, tricalcium aluminate, hydrogarnet, tetracalcium aluminate hydrate, etc., to form ettringite. Initially, calcium in the pore solution is supplied by Portlandite. When Portlandite is depleted from the system, calcium silicate hydrate dissociates to form calcium hydroxide and silica gel.

A geochemical speciation code, ORCHESTRA [5], is used in this work to calculate the equilibrium phases of the solids. The change in volume due to the dissolution and precipitation of solids is expressed as

$$\Delta V_s = \sum_{m=1}^{M} (V_m - V_m^{init}) \tag{2}$$

where M is the number of solid phases, and V_m^{init} and V_m are the initial and current volume of the mth solid. The volume of the solid is calculated by multiplying number of moles of each mineral obtained from the equilibrium calculations and molar volume of the respective mineral phase. If the final volume of solids is more than the initial volume, the additional volume can only be accommodated in the pore space. Thus the decrease in porosity is expressed as

$$\varphi = \varphi_0 - \frac{\Delta V_s}{V} \tag{3}$$

where φ and φ_0 are the current and the initial porosities respectively and V is the volume of the representative volume element. Similarly, if the final solid volume is less than the initial solid volume, porosity increases which can also be calculated from Eqs. (2) and (3). The change in diffusivity due to the change in porosity is calculated using an empirical equation given as [6]

$$H_D(\varphi) = \frac{e^{\frac{4.3\varphi}{V_p}}}{e^{\frac{4.3\varphi_0}{V_p}}} \tag{4}$$

where V_p is the volume of the paste. Eq. (4) is a correction factor which is multiplied with the diffusivity ($\frac{D_i^0\varphi}{\tau}$) in Eq. (1) and is used as the changed diffusivity for the next time step.

Damage accumulation

As mentioned in the previous subsection, if the final solid volume is more than the initial solid volume, the additional solid is accommodated in the pore space. The solid grows and eventually exerts pressure on pore wall of the surrounding cement matrix. Cracks start to form when the stress induced in the cement matrix exceeds the strength of the material. The solids deposited in the pores and the pores themselves are morphologically different. Thus the solids do

not have to fill up the total pore volume in order to start exerting pressure. Thus it is assumed that a fraction of the pore space (b) is available for solid product deposition before strain can develop. This is a model parameter which needs to be calibrated using experimental results. The net solid volume which contributes to the strain development is calculated as

$$\overline{\Delta V_s} = \Delta V_s - b\varphi V \tag{5}$$

The volumetric strain is calculated as

$$\bar{\varepsilon} = \frac{\overline{\Delta V_s}}{V} \tag{6}$$

if $\overline{\Delta V_s} > 0$. Otherwise it is zero. The uniaxial strain is calculated as

$$\varepsilon = \frac{\bar{\varepsilon}}{3} \tag{7}$$

assuming the structure to be homogeneous and isotropic. A continuum damage mechanics-based approach is used in this paper to relate the strain to the cracked state of the structure using experimental stress-strain curve of the material. The tensile stress-strain relation of cementitious materials exhibits three sequential regions – linear ascending, nonlinear ascending and nonlinear descending regions. There is no damage accumulation in the linear ascending region. In the nonlinear ascending region, a crack density parameter C_d that reflects accumulated damage can be expressed as

$$C_d = k\left(1 - \frac{\varepsilon^{th}}{\varepsilon}\right)^m \text{ for } \varepsilon > \varepsilon^{th} \tag{8}$$

where ε is the strain, ε^{th} is the threshold strain at which micro-cracks start forming and k and m are parameters that need to be calibrated from the experimental stress-strain diagram. The damage parameter ω can be conceptually defined as the ratio of damaged strength to the undamaged strength of the material. Assuming that the damage parameter is not affected by the Poisson's ratio of the damaged material, ω can be expressed as [7, 8]

$$\omega \approx \left({}^{16}/_{(9)C_d}\right) \tag{9}$$

The post-peak response of the material is modeled by using the relations [8, 9] given as

$$\frac{\sigma}{f_t'} = \sqrt{\frac{\tan\left(\frac{\pi\omega_0}{2}\right)}{\tan\left(\frac{\pi\omega}{2}\right)}} \tag{10}$$

$$\frac{w}{w_0} = \frac{\sigma}{f_t'} \frac{\log\left[\sec\left[\left(\frac{\pi\omega}{2}\right)\right]\right]}{\log\left[\sec\left[\left(\frac{\pi\omega_0}{2}\right)\right]\right]} - 1 \quad (11)$$

where σ is the stress, f_t' is the maximum tensile stress, ω_0 is the damage parameter at peak stress, w and w_0 are the current post-peak deformation and the deformation at the peak stress respectively. The damage parameter starts from 0 at the threshold strain (ε^{th}) and reaches 1 at failure. The maximum allowable value of damage parameter is assumed to be 0.9 in the numerical simulations presented in this paper to allow for additional uncertainties and margin in safety.

Change in diffusivity

The effect of development of strain on the formation of cracks is discussed in the previous subsection. The presence of cracks enhances diffusivity which leads to more diffusion of ions from outside into the structure (ingress) and more leaching out of ions from inside of the structure. When the cracks are dilute in concentration, the changed diffusivity is expressed as [10, 11]

$$D = \frac{H_D(\varphi)(D_i^0\varphi)}{\tau\left(1 + \frac{32}{9}C_d\right)} \quad (12)$$

When the microcracks coalesce and form macrocracks, the diffusivity is calculated using the following expression [11, 12]

$$D = \frac{H_D(\varphi)(D_i^0\varphi)}{\tau\left[\left(1 + \frac{32}{9}C_d\right) + \frac{(C_d - C_{dc})^2}{(C_{dec} - C_d)}\right]} \quad (13)$$

where C_{dc} is the conduction percolation threshold below which concentration of cracks is sparse and C_{dec} is the rigidity percolation threshold at which the cluster of cracks transects the volume. The values for the thresholds are obtained from the literature [10, 12, 13]. The model described in this section is calibrated and validated in [2].

SENSITIVITY ANALYSIS

Durability analysis of a structure using a numerical model depends on the knowledge of input and model parameters. Effects of three primary factors on the model response are assessed in this paper by performing sensitivity analysis. These factors are – (1) chemical equilibrium models comprised of different combinations of mineral phases and initial concentrations of ionic species,

(2) prescribed boundary conditions obtained from various literature sources, and (3) a mechanical parameter required for development of cracks.

Chemical equilibrium model

One of the key aspects of modeling chemical attack on the concrete structure is selection of a mineral set (i.e., a set of precipitation-dissolution reactions) that represents the chemical composition of the cementitious material, partitioning of chemical species between the pore solution and solid phases, and the minerals that may form as a result of chemical reactions. The effect of mineral sets on the model responses are assessed by comparing simulation results using the chemical equilibrium module with experimental data.

The experimental data of pH dependent solubility of various ionic species is obtained from a database/expert decision support system, LeachXS [14]. The database contains results of a large number of experiments performed on a range of cement and mortar compositions. Specimens are crushed to simulate a completely degraded state (95% of the material < 2 mm in size resembling a completely cracked specimen) and are allowed to leach while in contact with water under different pH conditions until solid-solution chemical equilibrium is approximated. In the U.S., this approach is being standardized for SW-846 as EPA Method 1313 [15]. It is assumed that the maximum leached amount as well as the maximum amount capable of reacting with the pore solution for a particular specimen (i.e., the available quantities) cannot exceed the amount obtained from the experiments. The LeachXS database in conjunction with the chemical equilibrium model in ORCHESTRA provides information regarding the mineral phases most likely to be present in the system and required to produce good agreement between the experimental results and model representation for solution concentration of the set of dissolved species (e.g., OH^-, Ca^{+2}, SO_4^{-2}, etc.) as a function of pH.

In this paper, the experimental data on a cementitious material similar in composition to the future vault concrete material [16, 17] is selected from the database and compared with the simulation results using different mineral sets. The two most promising mineral sets are chosen in this paper for comparison purposes after a preliminary investigation with several mineral sets. These are – (i) M1, selected by comparing experimental results and the simulation results for similar materials (see Table I) and (ii) M2, recommended in the literature for simulation of cementitious materials (see [18], [19]). The model results are also sensitive to the initial concentrations of the species. Therefore, two initial concentrations are selected to assess their effects on the simulation – (i) C1, available concentrations of the species obtained from the experiment (described above) and (ii) C2, total concentrations of the species calculated from the composition of cement and cement admixtures [17]. Figure 1 shows the comparison of the experiment with the simulation results for four cases – (i) M1-C1, (ii) M1-C2, (iii) M2-C1, and

(iv) M2-C2. Error is estimated as the difference between numerical simulation and the experimental data as reported in Table II. It can be observed from the values given in the table that the total error is minimum in the case of M1-C1. Therefore M1 mineral set and C1 initial concentrations are used in the rest of the paper for sensitivity analyses. In Table II, M1*-C1 represents the error in the calibrated best fit model response with respect to the experimental results and the detailed explanation is given in the next Section.

The above mentioned four cases are also used in the coupled model (i.e., reactive transport and damage) to simulate the rates of damage progression as shown in Figure 2. One end of a 200 mm thick concrete wall (thickness of the future vault wall [20]) is in contact with sulfate containing pore solution of low activity nuclear waste having sulfate concentration of 250 mmol/L [21]. The porosity and tortuosity of the structure are 0.1 and 430 [17, 22]. The structure is divided into 100 cells and one cell is assumed to have cracked completely when the damage parameter (described in the previous section) reaches the maximum allowable value (= 0.9 in this paper). The fraction of porosity available for solid product deposition (b) is assumed to be 0.3 which is the median value reported in the literature [23]. The numerical simulations were performed for 100 years and the progressions of damage are plotted as a function of time. The time to complete cracking/damage of the structure is obtained by extrapolating the damage progression trend to the time when damage has progressed completely through the thickness of the structure. It can be observed from the figure that the rates of damage progression are significantly dependent on the mineral sets and the initial concentrations of species. The times to complete damage are estimated to be 209, 1190, 239 years and infinity (no damage observed) for the above mentioned 4 cases respectively. It is important to note that M1-C1 is the most conservative case among the four cases as the most aggressive damage is observed in this case. Thus the selection of mineral set is an essential step in the numerical simulation of chemical attack on the cementitious materials.

Table I: Mineral phases chosen for sensitivity analysis.

Mineral Phase	Expanded Formula	Common Name
$C_{1.67}SH_{2.1}$	$1.67CaO.SiO_{2.2.1H_2O}$	Jennite
$C_{0.83}SH_{1.3}$	$2CaO.2.4SiO_{2.3.2H_2O}$	Tobermorite-II
C_2ASH_8	$2CaO.Al_2O_3.SiO_{2.8H_2O}$	Stratlingite
C_2FSH_8	$2CaO.Fe_2O_3.SiO_{2.8H_2O}$	Fe-Stratlingite
C_3AH_6	$3CaO.Al_2O_{3.6H_2O}$	Hydrogarnet
C_3FH_6	$3CaO.Fe_2O_{3.6H_2O}$	Fe-Hydrogarnet
$Al(OH)_3$ (amorphous)	-	Gibbsite
$Mg(OH)_2$	-	Brucite
M_4ACH_8	$4MgO.Al_2O_3.CO_{2.8H_2O}$	CO_3-Hydrotalcite
$CaO.CO_2$	-	Calcite
$C_6A\bar{S}H_{32}$	$6CaO.Al_2O_{3.32H_2O}$	Ettringite
$C_6F\bar{S}H_{32}$	$6CaO.Fe_2O_{3.32H_2O}$	Fe-Ettringite
$Fe(OH)_3$ (microcrystalline)	-	Ferric Hydroxide

CSH_2	$CaO.SO_{3.2H_2O}$	Gypsum
CH	$CaO.H_2O$	Portlandite
S	SiO_2	Silica
$NaAlSi_3O_8$	-	Albite

Table II: Error between experiment and model.

Cases	Error prediction in:						
	Al^{+3}	Ca^{+2}	Fe^{+3}	Mg^{+2}	H_4SiO_4	SO_4^{-2}	Total
M1-C1	**2.42**	**1.17**	**1.43**	**1.47**	**1.85**	**1.11**	**9.44**
M1-C2	2.49	1.53	2.53	1.39	2.93	1.99	12.85
M2-C1	4.15	1.39	4.34	1.75	1.99	0.44	14.06
M2-C2	3.30	2.82	3.83	3.46	3.60	1.99	19.00
$M1^*$-C1	2.14	0.74	1.08	0.95	1.89	0.85	7.64

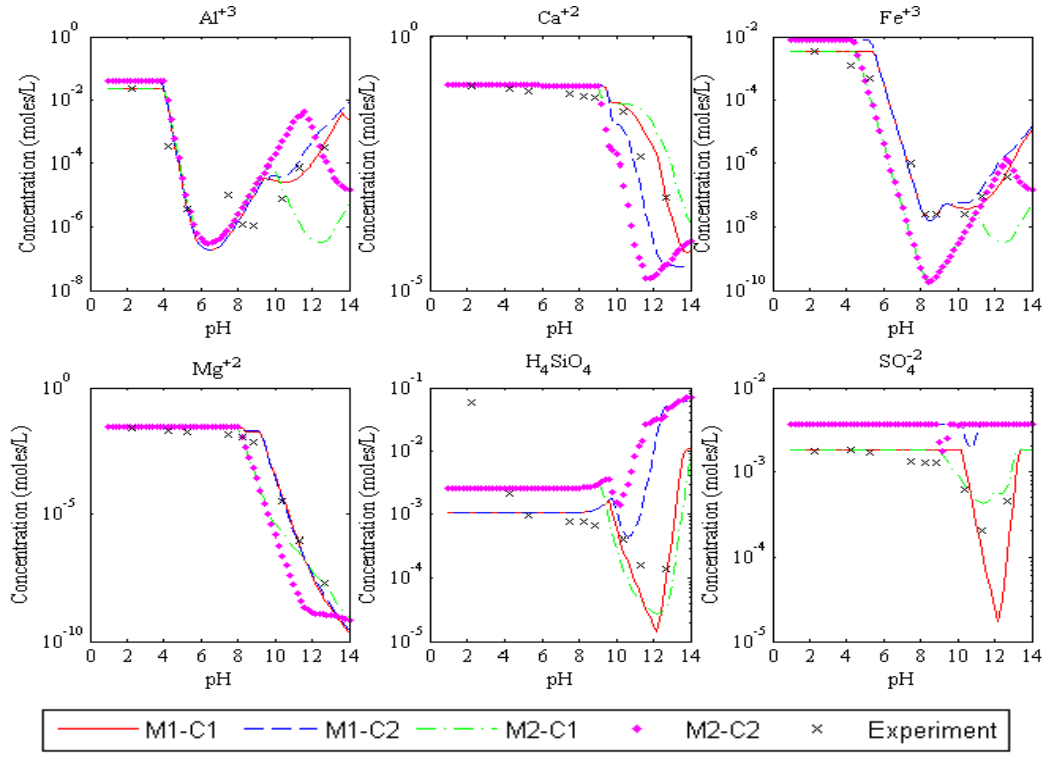

Figure 1: Effect of mineral sets and initial concentrations on the model response.

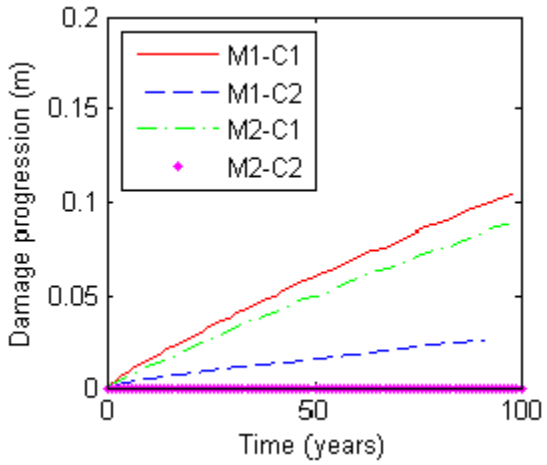

Figure 2: Effect of mineral sets and initial concentrations on damage progression.

Boundary condition

In this subsection, sensitivity of the model response with respect to the boundary condition is assessed by performing simulations with three selected boundary conditions. As before, one end of a 200 mm thick concrete wall is exposed to sulfate rich solution and *b* is 0.3. The selected sulfate concentrations at the boundary are – (i) 250 mmol/L (24000 mg/L) [21], (ii) 120 mmol/L (11520 mg/L) [24], and (iii) 56 mmol/L (5376 mg/L) [24]. The M1 mineral set and C1 initial concentrations of species are used from the previous subsection. Figure 3 shows the trends in the damage progression. The extrapolated times to complete damage are estimated to be 209, 380 and 786 years for the three cases mentioned above and it is evident that the durability estimations are significantly affected by the boundary sulfate concentrations. Therefore, accurate estimation of the waste form pore solution sulfate concentration is needed for an efficient design of the future containment structures.

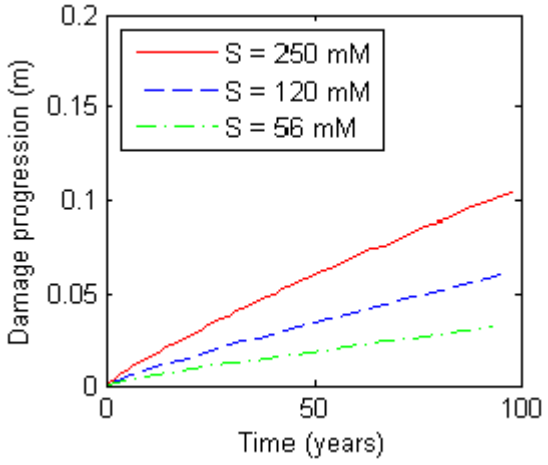

Figure 3: Effect of sulfate concentration on damage progression (b = 0.3).

Mechanical parameter

One of the most significant parameters in durability analysis using the numerical model described in the last section is the fraction of porosity available for solid product deposition, (b in Eq. (5)). This is essentially a model parameter that needs to be calibrated using experimental data which is often not available for real application cases. In this subsection, effect of the parameter is assessed by performing numerical simulations with three selected values – 0.2, 0.3 and 0.4 i.e., ± 0.1 with respect to the median value, 0.3 [21]. The simulations are performed for the 200 mm thick concrete wall exposed to 120 mmol/L of sulfate solution at one end with the mineral set and initial concentrations selected before. Figure 4 shows that the rate of damage progression is slower for higher availability of pore space. The times to complete damage of the structure are extrapolated to be 258, 380 and 606 years for the three selected cases respectively, and it is evident that the durability analysis is significantly affected by the parameter. Thus accelerated tests on the material of interest are required to estimate mechanical properties of the structure for a more accurate assessment of durability and subsequent design of the future containment structure.

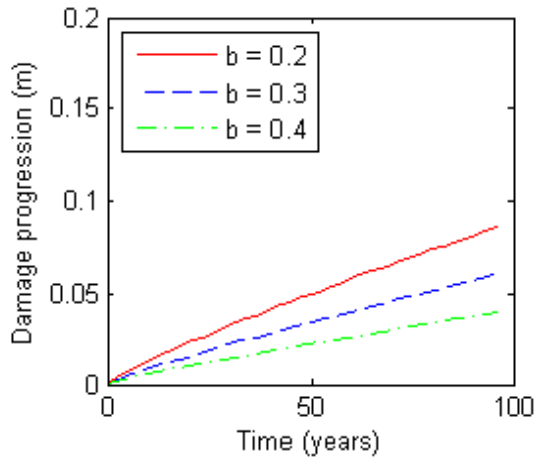

Figure 4: Effect of available fraction of porosity on damage progression (S = 120 mmol/L).

PROBABILISTIC DURABILITY ANALYSIS

The numerical model described in this paper for assessing damage progression through a cementitious structure under external sulfate attack requires several input and model parameters. These parameters can be obtained from the experiments or from the literature. In either case, the values of the parameters will have some uncertainty associated with them, leading to uncertainty in the model response. There are mainly three sources of uncertainty – (i) physical variability due to the inherent randomness of the variables, (ii) data uncertainty due to sparse or interval data, and (iii) model uncertainty due to assumptions and approximations used during the modeling process. Various methods are available in the literature for quantifying the uncertainty in the parameters and propagating it through the model, leading to the quantification of uncertainty in

the model prediction. The integrated effect of uncertainty in various parameters of the model is assessed in this section by performing probabilistic durability analysis.

The physical variations in the parameters are incorporated by defining them as random variables with probability density functions (PDFs) e.g. external sulfate concentration, Young's modulus etc. (Table III) . The data uncertainty is assumed to be coming from small number of samples used to estimate some parameters, e.g., porosity, tortuosity etc. These parameters are modeled as distributions with uncertain parameters. One approach for constructing distributions of distribution parameters having an underlying normal population is as follows: let X be a sample set of size n that is assumed to have an underlying normal distribution with true but unknown mean and variance μ and σ^2 respectively. The sample mean and variance calculated from X are $\bar{x}$ and $\bar{s}^2$ respectively. Then, $\frac{\bar{x}-\mu}{\frac{\bar{s}}{\sqrt{n}}}$ and $\frac{(n-1)\bar{s}^2}{\sigma^2}$ are observed to have the *student's t* distribution and *chi-square* distribution with $n-1$ degrees of freedom respectively [25]. This approach is used in this section with the assumption that only 5 samples were available for estimation of the selected parameters.

It is important to acknowledge that there is uncertainty associated with the input parameters of the chemical equilibrium model (i.e., thermodynamic constants) and the experimental data used for selecting the mineral set. Additionally, there are various assumptions and approximations in the model that add to the overall uncertainty. Thus it is important to quantify uncertainty in the chemical reaction module so that the total uncertainty in the model prediction can be quantified. A Bayesian calibration method is applied in this paper using model M1-C1 as the initial base model to obtain the distributions of the equilibrium constants (i.e., the model parameters) subjected to the uncertainty in the input parameters and the experimental measurements. Then the best set of equilibrium constants are obtained from the calibrated distributions that results in the minimum error between the simulation results and the experimental data (given in Table II). It can be observed from Table II that the error in the model prediction with the calibrated best fit equilibrium constants (M1*-C1) is less than the error in model prediction with the equilibrium constants obtained from the literature (M1-C1). Figure 5 shows examples of the prior and the posterior distributions, prior mean values and the calibrated best fit values. It is important to note that this approach allows estimation of the distributions of the equilibrium constants representing uncertainty in the parameters due to uncertainty in the input parameters, experimental measurements and various assumptions and approximations in the model. The same approach can also be used to quantify model uncertainty in the transport and the damage modules if corresponding experimental data are available.

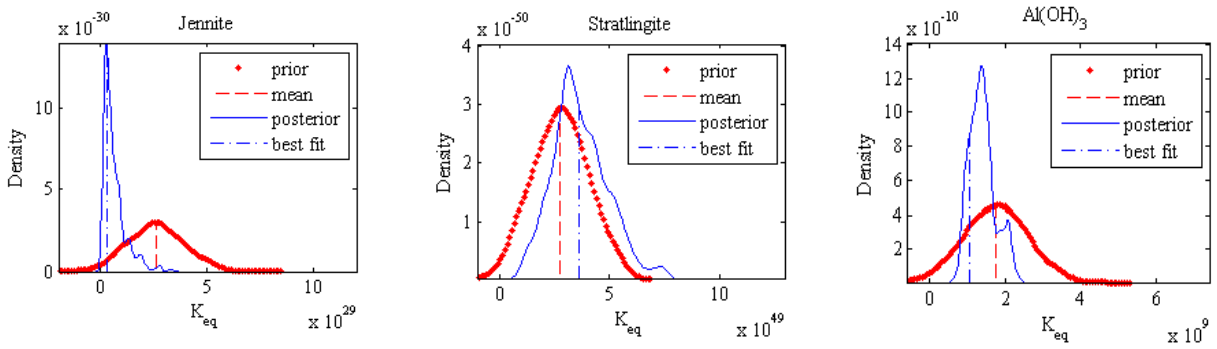

Figure 5: Examples of the prior and posterior distributions.

Finally, a single-loop Monte Carlo simulation technique is used to assess the integrated effect of physical and chemical parameter uncertainty in various parameters of the model on the durability assessment. The 200 mm thick concrete wall is exposed to sulfate solution at three concentrations with associated uncertainty for the purpose of illustration (Table III).

Table III: Statistical descriptions of the model and input parameters.

Parameter	**Statistical Description**
Porosity of concrete wall	$N(\mu_1, \sigma_1)$ $\frac{0.1-\mu_1}{\frac{5e\text{-}3}{\sqrt{5}}}$ ~Student's t with 4 degrees of freedom $\frac{4*(5e\text{-}3)^2}{\sigma_1^2}$ ~Chi-square with 4 degrees of freedom
Tortuosity of concrete wall	$N(\mu_2, \sigma_2)$ $\frac{430-\mu_2}{\frac{64.5}{\sqrt{5}}}$ ~Student's t with 4 degrees of freedom $\frac{4*(64.5)^2}{\sigma_2^2}$ ~Chi-square with 4 degrees of freedom
Initial Young's Modulus (MPa)	$N(37.5e3, 4e3)$
Ultimate Tensile Strength (MPa)	$N(5.1, 0.3*5.1)$
Fraction of available porosity	$N(0.3, 0.1*0.3)$
External sulfate concentration (moles/L)	$N(0.25, 0.1*0.25)$, $N(0.12, 0.1*0.12)$, $N(0.056, 0.1*0.056)$
Total concentrations of species (moles/kg)	$N(\mu_i, \sigma_i)$

	$\frac{\bar{x}_i - \mu_i}{\frac{s_i}{\sqrt{5}}}$ ~Student's t with 4 degrees of freedom $\frac{4 * (s_i)^2}{\sigma_i^2}$ ~Chi-square with 4 degrees of freedom $\bar{x}_i$: LeachXS database s_i : 0.1*$\bar{x}_i$
Equilibrium constants	As calibrated

Note: *N(a, b)* represents normal distribution with mean *a* and *b* standard deviation.

The times required for complete cracking/damage are calculated from 50 realizations of the random parameters for each boundary condition and the cumulative probabilities of complete cracking are estimated as shown in Figure 6. The mean time to failure is estimated to be approximately 1000 years. The times to complete damage at selected percentile values are given in Table IV. In this respect, it is important to acknowledge that considerable amount of experimental data are required to accurately estimate the model parameters and to validate various parts of the numerical model. However, numerical simulation results as given in Figure 6 can provide useful insights for designing a future structure, maintenance scheduling and monitoring an existing or future structure.

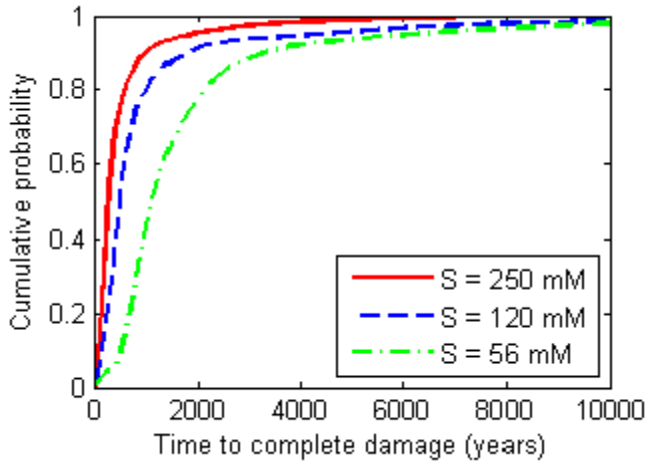

Figure 6: Cumulative probability of time to complete damage.

Table IV: Time (years) to complete damage at selected percentiles.

Cases / Percentiles	Case 1 S = 250 mM	Case 2 S = 120 mM	Case 3 S = 56 mM
5th	78	109	338
25th	186	318	772

50th	285	508	1135
75th	513	835	1849
95th	1886	4354	6120

CONCLUSIONS

A numerical model for degradation assessment of cementitious materials under external sulfate attack is described in this paper by combining a reactive transport model with a continuum damage mechanics based model. Effects of various parameters on the durability assessment have been evaluated using the numerical model. The mineral set and initial concentrations of species resulting in minimum error with respect to experimental results also results in the most aggressive damage scenario. Sulfate concentration at the boundary and the fraction of available porosity significantly affect the durability. EPA leaching assessment method 1313, estimation of porosity, tortuosity and external boundary condition, and mechanical stress-strain diagram provide useful information that can be used to reduce model uncertainty. Experimental approaches are needed to estimate fraction of porosity available for solid product deposition and verify the rate of damage progression. Overall, the sensitivity analysis shows that the damage progression can be controlled by adjusting (i) concrete composition, and (ii) sulfate boundary condition.

The chemical reaction model and EPA method 1313 experimental data were used to estimate uncertainty in the equilibrium constants using a Bayesian calibration method. The coupled numerical model was then used to demonstrate application of the durability analysis framework considering uncertainty in the selected physical and chemical parameters. Statistical representations of the parameters were incorporated in the durability assessment framework, allowing the development of the probability distribution of time to complete damage using a single loop Monte Carlo simulation technique. The sensitivity analysis and the probabilistic durability analysis used in conjunction with the described model can provide useful insights for evaluating potential designs for life extension of existing and future containment structures and to achieve desired performance objectives.

ACKNOWLEDGEMENTS

This paper was prepared with financial support by the U. S. Department of Energy, under Cooperative Agreement Number DE-FC01-06EW07053 entitled 'The Consortium for Risk Evaluation with Stakeholder Participation III' awarded to Vanderbilt University and support to the Savannah River National Laboratory, Savannah River Nuclear Solutions, LLC under Contract No. DE-AC09-08SR22470 with the U.S. Department of Energy. This research was carried out as part of the Cementitious Barriers Partnership supported by U.S. DOE Office of Environmental Management. The opinions, findings, conclusions, or recommendations expressed herein are those of the authors and do not necessarily represent the views of the Department of Energy or Vanderbilt University.

REFERENCES

1. J.R. Clifton, J.M. Pommersheim, Sulfate attack of cementitious materials: volumetric relations and expansions, Gaithersburg, MD, Building and Fire Research Laboratory, National Institute of Standards and Technology, 1994.
2. S. Sarkar, S. Mahadevan, J.C.L. Meeussen, H. van der Sloot, D.S. Kosson, Numerical simulation of cementitious materials degradation under external sulfate attack, Cement and Concrete Composites, 32, p. 241-252, 2010.
3. E. Samson, G. Lemaire, J. Marchand, J.J. Beaudoin, Modeling chemical activity effects in strong ionic solutions, Computational Materials Science, 15, p. 285-294, 1999.
4. J. Marchand, E. Samson, Y. Maltais, J.J. Beaudoin, Theoretical analysis of the effect of weak sodium sulfate solutions on the durability of concrete, Cement and Concrete Composites, 24, p. 317-329, 2002.
5. J.C.L. Meeussen, ORCHESTRA: An object-oriented framework for implementing chemical equilibrium models, Environmental Science and Technology, 37, p. 1175-1182, 2003.
6. E. Samson, J. Marchand, Modeling the transport of ions in unsaturated cement-based materials, Computers & Structures, 85, p. 1740-1756, 2007.
7. B.L. Karihaloo, Fracture mechanics and structural concrete, Longman Scientific and Technical, Essex, England, 1995.
8. B. Budiansky, R. O'Connell, Elastic moduli of a cracked solid, International Journal of Solids and Structures 12, p. 81-97, 1976.
9. R. Tixier, B. Mobasher, Modeling of damage in cement-based materials subjected to external sulfate attack. I: formulation, Journal of Materials in Civil Engineering 15, p. 305-313, 2003.
10. D. Krajcinovic, M. Basista, K. Mallick, D. Sumarac, Chemo-micromechanics of brittle solids, Journal of the Mechanics and Physics of Solids 40, p. 965-990, 1992.
11. M. Basista, W. Weglewski, Micromechanical modeling of sulphate corrosion in concrete: influence of ettringite forming reaction, Theoretical and Applied Mechanics, 35, p. 29-52, 2008.
12. E. Charlaix, Percolation threshold of a random array of discs: a numerical simulation, Journal of Physics A: Mathematical and General, 19, p. L533-L536, 1986.
13. D. Sornette, Critical transport and failure in continuum crack percolation, Journal de Physique, 49, p. 1365-1377, 1988.
14. van der Sloot, H.A., Seignette, P., Comans, R.N.J., van Zomeren, A., Dijkstra, J.J., Meeussen, H., Kosson, D.S., Hjelmar, O., Evaluation of environmental aspects of alternative materials using an integrated approach assisted by a database/expert system, in Advances in Waste Management and Recycling, Dundee, Scotland, 2003.
15. Garrabrants, A.C., Kosson, D.S., van der Sloot, H.A., Sanchez, F., Hjelmar, O., Background Information for the Leaching Environmental Assessment Framework (LEAF) Test Methods. USEPA, Office of Research and Development, 2010.
16. Phifer, M.A., Millings, M.R., Flach, G.P., Hydraulic property data package for the E-area and Z-area soils, cementitious materials, and waste zones, 2006.
17. SIMCO Technologies, I., Evaluation of sulfate attack on saltstone vault concrete and saltstone, Ed. C.A. Langton, Savannah River National Laboratory, Aiken, SC, 2008.
18. Lothenbach, B., Matschei, T., Moschner, G., Glasser, F.P., Thermodynamic modelling of the effect of temperature on the hydration and porosity of Portland cement. Cement and Concrete Research, 38, p. 1-18, 2008.

19. Lothenbach, B., Winnefeld, F., Thermodynamic modeling of the hydration of Portland cement, Cement and Concrete Research, 36, p. 209-226, 2006.
20. Flach, G.P., Jordan, J.M., Whiteside, T., Numerical flow and transport simulations supporting the saltstone disposal facility performance assessment, SRNL-STI-2009-00115, June 2009.
21. Langton, C.A., Analysis of saltstone pore solutions - PSU progress report IV. 1987, E. I. du Pont de Nemours and Company: Aiken, South Carolina.
22. Dixon, K., J. Harbour, and M.A. Phifer, Hydraulic and physical properties of saltstone grouts and vault concretes, 2008.
23. Denham, M., Thermodynamic and mass balance analysis of expansive phase precipitation in saltstone, WSRC-STI-2008-00236, May 2008.
24. SIMCO Technologies, I., Demostration of STADIUM for the performance assessment of LAW structures, 2010.
25. Haldar, A. and S. Mahadevan, Probability, Reliability, and Statistical Methods in Engineering Design. 2000: John Wiley and Sons.